Asian Journal of Chemistry; Vol. 35, No. 11 (2023), 2733-2738

ASIAN JOURNAL OF CHEMISTRY

https://doi.org/10.14233/ajchem.2023.30266

Graphene Oxide-based Gel as Potential Nanomaterial for Sustained Release of an Anticancer Drug

ABHIJIT BISWAS

Department of Chemistry, Krishnagar Government College, Krishnagar-741101, India

Corresponding author: E-mail: biswas.abhijit5@gmail.com

Received: 10 August 2023; *Accepted*: 24 September 2023; *Published online*: 31 October 2023; AJC-21429

A new graphene oxide-based gel comprised of mitoxantrone an anticancer drug and graphene oxide has been synthesized in water at room temperature. This gel-based soft material was formed due to the supramolecular interactions including hydrogen bonding, acid–base and π–π stacking. Transmission electron microscopy, atomic force microscopy, X-ray diffraction and rheological studies have been employed to characterize the gel. By introducing a small quantity of Ca^{2+} ions at room temperature, this hybrid gel can effectively facilitate the sustained and controlled release of mitoxantrone drug. The release of the drug molecules was checked and discussed using UV-visible spectroscopic analyses. With the advantages of this graphene oxide-based gel, the soft gel-based material could be a soft drug-releasing agent.

Keywords: Graphene oxide, Gel, Controlled release, Anticancer drug, Mitoxantrone.

INTRODUCTION

Self-assembly stands out as a highly valuable method for integrating diverse nanoscale constituents into macroscopic materials endowed with intriguing characteristics. The most prevalent instances of self-assembling systems are gel formations, which arise from the non-covalent interactions of small molecules [1-3]. Within the intriguing realm of soft materials, these supramolecular gels occupy a distinctive category, characterized by the assembly of gelator molecules that form a network structure capable of immobilizing a substantial quantity of solvent molecules. These gels find valuable utility across a range of fields, such as tissue cultures, material engineering, light harvesting, regenerative medicine, controlled drug release and addressing oil-spill cleanup challenges [4-7]. Certain gel matrices have been employed in the development of hybrid gels incorporating graphene [8-11]. The exceptional electronic, mechanical and optical properties of graphene make graphene-based materials exceedingly promising for a wide range of potential applications across diverse fields [12-24]. One of the interesting properties of graphene is the adsorption of organic molecules [25,26].

Owing to the large polyaromatic surface and hydrophilic functional groups, the graphene sheets have the capacity to enhance the adsorption of a huge number of molecules through hydrogen bonding and π–π interactions. These adsorption techniques lead to the application of the removal of dyes from wastewater and the release of antitumor drugs [27-29]. The main advantage of using graphene is the simplicity of operation. Recently, Kim *et al*. [30] developed hydrogels based on graphene, demonstrating outstanding capacity for removing methylene blue and rhodamine B dyes. Zhang *et al*. [31] reported the doxorubicin hydrochloride containing graphene oxide-based gel that can release the doxorubicin hydrochloride in a controlled manner. There are several graphene-based hybrid systems have been found in the literature that shows the sustained release of doxorubicin hydrochloride [32,33]. In this report, mitoxantrone containing graphene oxide (GO) based gel-phase materials (GO-MTX) have been synthesized. Graphene oxide (GO) features an abundance of hydrophilic groups, including hydroxyl and carboxylic moieties, while its polyaromatic surface allows for noncovalent interactions with mitoxantrone. This leads to the formation of gel in aqueous medium. It is widely recognized that the carboxyl group can effectively bind to the calcium ion [34]. A novel approach described by Ruoff *et al*. [35] where the epoxide and hydroxyl functional groups on the basal planes and the carboxylate moieties on the edges of GO interact with Ca^{2+} ions and enhance

the mechanical strength of the hybrid material. There-fore, it can be stated that GO is one of the powerful candidates for interaction with Ca^{2+} ions. By adopting such properties of GO, herein, for the first time, the calcium ion has been used for sustained and controlled release of mitoxantrone drug from GO-based gel. The concentration of calcium ions affects the releasing rate of the drug molecules from the GO-based gel.

EXPERIMENTAL

All the chemicals *viz.* potassium permagnate, sodium nitrate, calcium chloride, hydrogen peroxide, ammonia and solvents were procured from SRL, India, while graphite powder and mitoxantrone were acquired from Sigma-Aldrich, India. For all experiments, Ultra Pure Milli-Q grade water was employed exclusively.

Preparation of graphene oxide (GO): Graphene oxide (GO) was synthesized from natural graphite powder (< 30 µm) according to modified Hummers & Offeman's method [36]. Initially, 0.62 g of graphite powder was mixed with 25 mL of conc. H_2SO_4, maintaining continuous stirring. Subsequently, 0.3 g of $NaNO_3$ was introduced and cooled the mixture to 0 ºC. While vigorously agitating, 1.87 g of $KMnO_4$ was gradually added, ensuring the temperature remained below 20 ºC to prevent overheating. The resulting mixture was then transferred to a 35 ºC water bath and stirred for 30 min, forming a brownish-grey paste. Next, the mixture was diluted by the addition of 37 mL of water, gradually increasing the temperature to 90 ºC and maintaining it for 15 min. To complete the reaction, 30% H_2O_2 (0.6 mL) was mixed to it. The warm solution underwent thorough washing with HCl and warm water and the resulting solid was dispersed in 100 mL of distilled water through sonication. Afterwards, centrifuged the solution at 3000 rpm for 15 min, followed by re-suspension through sonication and subsequent centrifugation at 20000 rpm. This centrifugation process was repeated multiple times. Finally, the centrifuged viscous graphene oxide was collected and freeze-dried it under vacuum conditions to obtain a solid powder.

Preparation of GO-based gel: A stock solution of mitoxantrone was prepared with a concentration of 1.84 mg/mL by dissolving it in Milli-Q water. In standard procedure, sonication was employed to disperse GO in water, yielding a thick solution. Subsequently, 0.2 mL of drug solution was introduced into 0.8 mL GO dispersion, followed by sonication to obtain a gel based on GO. The resulting gel had a GO concentration of 2.8 mg/mL.

Drug release study: At first, three different Ca^{2+} solution of concentration 0.98 mg/mL, 1.4 mg/mL and 2.1 mg/mL were prepared by dissolving required amount of $CaCl_2$ in water. Then 200 µL of each solution added separately to the gel for drug release experiment.

Detection method: The X-ray diffraction analyses were conducted by placing them on glass plates and allowing them to air dry at room temperature over several days. Subsequently, the experiments was performed using a Bruker AXS X-ray diffractometer (Model no. D8 Advance) operating at 40 kV voltage and 40 mA current, utilizing Ni-filtered Cu$K\alpha$ radiation. Prior to the analysis, the instrument was calibrated with a standard Al_2O_3 (corundum) sample. For the measurements, a LynxEye super speed detector was employed with a scan speed of 0.3 s and a step size of 0.02º. For the rheological experiment, two distinct solutions: gel M with a concentration of 2.61% (w/v) and gel M′ with a concentration of 2.78% (w/v) were prepared. In these gels, the mitoxantrone concentrations were 1.84 mg/mL and 2.7 mg/mL, respectively. The rheological study was conducted using an AR 2000 advanced rheometer from TA Instruments, employing cone-plate geometry within a Peltier plate system. The cone had a diameter of 40 mm, an angle of 1º59′50″ and a truncation of 56 µm. For angular frequency sweep experiments, sweeps from 7 to 206 rad/s was performed while maintaining a fixed strain of 0.01% at 25 ºC. To explore the morphology transmission electron microscopy (TEM) and tapping-mode atomic force microscopy (AFM) were carried out. For TEM investigations, a drop of the diluted gel-phase material was applied to a TEM grid (300 mesh Cu grid) coated with Formvar and a carbon film, followed by vacuum drying at room temperature for 2 days. Imaging was carried out using a JEOL electron microscope, operating at an accelerating voltage of 200 kV. AFM study was carried out by placing a small quantity of wet hydrogel on mica and allowing it to dry slowly through air evaporation and subsequent vacuum drying at room temperature for 2 days. Imaging was performed using an Autoprobe CP Base Unit di CP-II instrument (model no. AP-0100). To examine the UV-vis absorption spectra of the released drug (mitoxantrone) solution in water, a Varian Cary 50 Bio UV-vis spectrophotometer was used at room temperature.

RESULTS AND DISCUSSION

Graphene oxide (GO) is a two-dimensional nanomaterial, that can readily exfoliate into a stable monolayer sheet and is dispersible in water, primarily attributed to the hydrophilic oxygenated functional groups (–OH) decorating its basal planes, alongside carboxylate groups (–COOH) lining the sheet's edges. Nevertheless, electrostatic repulsion between GO sheets arises due to the ionized carboxyl groups, thwarting their assembly in aqueous environments. However, when exposed to external molecules, the functional groups of GO can establish hydrogen bonding interactions and/or π–π interactions under specific conditions, thereby facilitating the assembly of GO sheets into gel structures. These external molecules can be termed cross-linking or binding agents. In this particular investigation, mitoxantrone, an anticancer drug has been introduced as a cross-linking or binding agent into GO dispersions in an aqueous medium, ultimately leading to the formation of stable hydrogels at room temperature (Fig. 1). Mitoxantrone possesses both -NH and -OH functional groups, enabling interactions with the -OH and -COOH as well as epoxide groups present on GO sheets through hydrogen bonding. Additionally, this drug holds aromatic moieties that can establish robust π–π stacking interactions with the polyaromatic surface of GO sheets. The observed minimum gelation concentrations at 1.86% (w/v) imply that mitoxantrone serves as an effective crosslinker/binder between GO sheets, facilitated by a combination of hydrogen bonding and π–π stacking interactions. This network, composed of GO and mitoxantrone molecules, can effectively immobilize water molecules, forming a stable gel matrix.

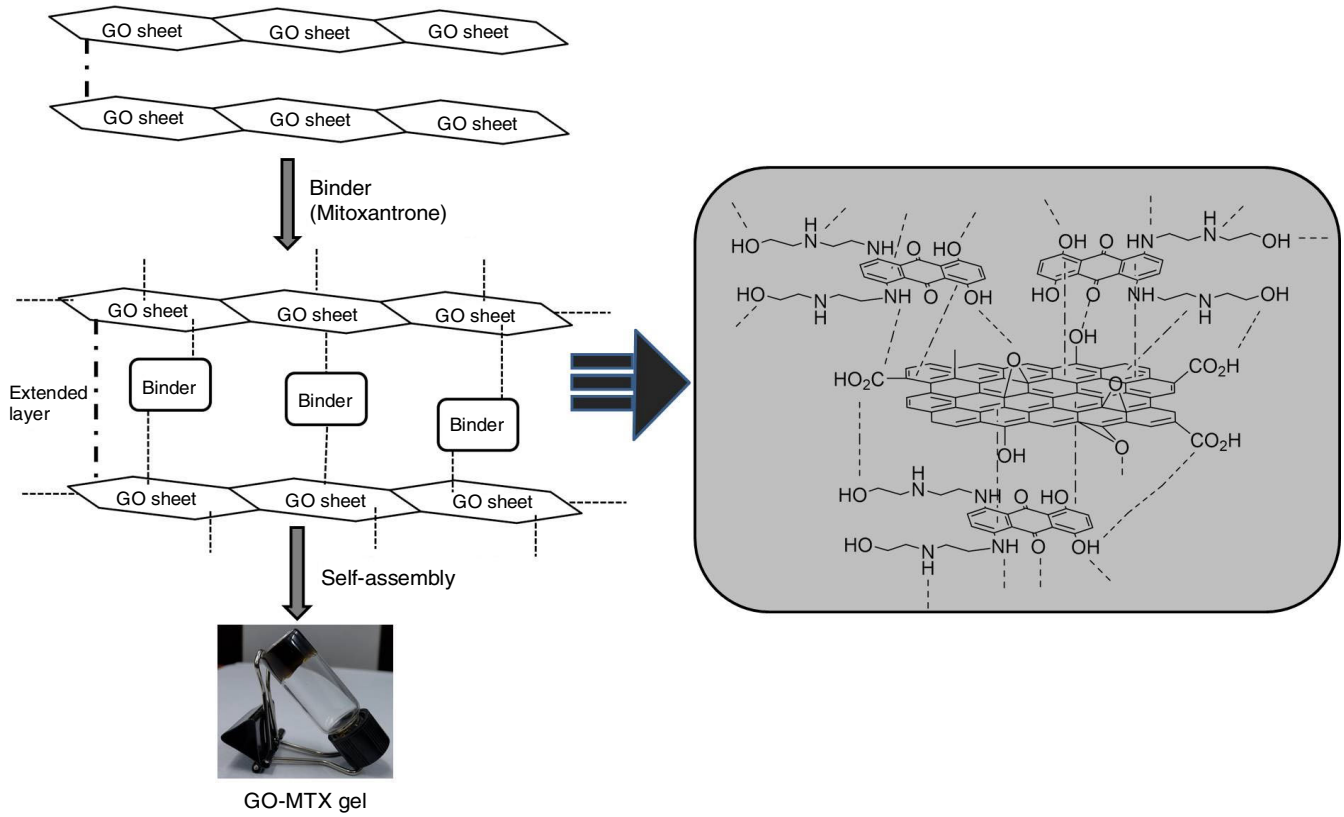

Fig. 1. Visual representation illustrating the creation of a physical gel and mode of interaction between GO and mitoxantrone

Rheological studies: To investigate the viscoelastic properties of gel, a rheological analysis was conducted at two different concentrations of the gel. During a frequency sweep experiment, the changes in the storage modulus (G′) and loss modulus (G″) was monitored while maintaining a constant strain of 0.1%. It is observed that G′ reflects the gel's ability to regain its original shape after deformation, while G″ indicates its propensity to flow. In the case of an ideal liquid, G′ equals 0, whereas for an ideal solid, G″ is 0. For a gel-phase material, G′ surpasses G″ and when the gel transitions into a sol state, G′ becomes equal to G″. In sol state, G″ exceeds G′. In GO-MTX gel, the gel strength depends on the number of binder (mitoxantrone) molecules present in the gel. The higher G′ values (58.7 KPa) of gel M′ (2.78%, w/v) than gel M (2.61%, w/v; G′ values at 43.4 KPa) at a fixed angular strength of 176 rad/s (Fig. 2) was due to the significant enhancement of the interaction of GO sheet with binder molecules. Furthermore, in both of these gels, the G′ value consistently surpasses the G″ value across the entire range of experimental frequencies. This observation suggests that mitoxantrone effectively establishes a physical gel and the gel's rigidity can be attributed to the presence of a greater number of interactions.

XRD studies: The distinct X-ray diffraction (XRD) patterns of lyophilized GO reveal a peak at 2θ = 10.01°, indicative of an interplanar spacing approximately measuring 8.86 Å (greater than that of natural graphite) as illustrated in Fig. 3a. This expansion in interlayer spacing results from the intercalation of oxygen-containing functional groups into the layers, leading to the disruption of the original crystal structure found in natural

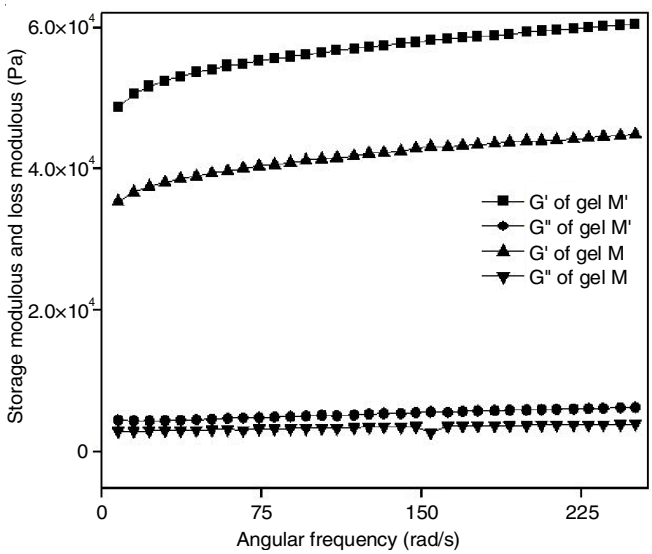

Fig. 2. Variations in the dynamic storage modulus (G′) and loss modulus (G″) of the GO-MTX gel as a function of frequency (The mitoxantrone concentration in M′ is higher than in M)

graphite samples [37]. The XRD patterns of the GO-MTX gel is different from those of pure GO. The diffraction peaks of the GO-MTX gel at 2θ = 9.87°, correspond to the inter-planar spacing of around 8.98 Å. The peak shift primarily arises from the absorption of mitoxantrone onto GO sheets. These observations, such as blue shift in the diffraction peak, provide evidence for the strong interaction between GO and mitoxantrone, causing a minor extension of the interplanar spacing within GO.

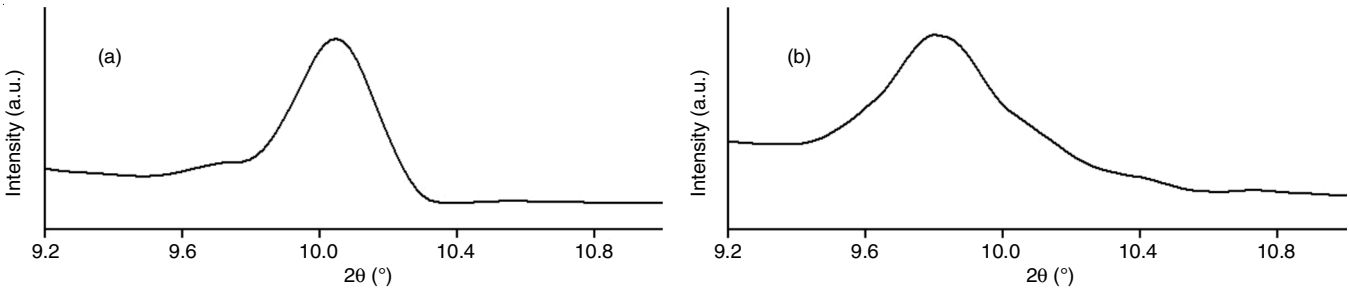

Fig. 3. XRD pattern of (a) GO and (b) GO-MTX gel in dried condition

Morphological characterizations: An examination of the gel-phase material morphologies within the GO-MTX gel was conducted using transmission electron microscopy (TEM) and atomic force microscopy (AFM). Fig. 4a illustrates the TEM image displaying self-assembled large nanosheet structures and Fig. 4b shows the AFM image revealing the formation of three-dimensional sheets. Additionally, nanofibers are also evident, predominantly adhering to the GO sheets, which are interconnected to form an extensive 3D network-like structure. These remarkable structural transformations are driven by the interactions, encompassing hydrogen bonding, π–π stacking and acid-base type electrostatic interactions.

Formation of gel: An attempt has been made to interpret the formation of gel. Graphene oxide (GO) is a 2D nanomaterial that contains (i) oxygenated functional groups (–OH, epoxide) on the basal planes; (ii) carboxylate groups (–COOH) on the edges; and (iii) large polyaromatic groups. These functionalities are capable of forming interactions with mitoxantrone molecules. Mitoxantrone contains multiple nitrogen (N)-containing functional groups (–NH) and hydrophilic oxygenated functional groups (–OH), in addition to its aromatic functionality. These –NH groups within mitoxantrone are capable of accepting protons from the –COOH groups present on the GO sheets, thereby forming acid–base-type electrostatic interactions. Furthermore, the –NH and –OH functionalities of mitoxantrone engage in the formation of hydrogen bonds with the hydroxyl (–OH) and epoxide groups on the GO sheets. Moreover, the aromatic groups of mitoxantrone engage in π–π stacking interactions with the polyaromatic groups found on the GO sheets. Consequently, the GO-MTX gel exhibits three distinct types of interactions, namely hydrogen bonding, acid–base and π–π stacking. This unique combination of interactions allows mitoxantrone to act as a binder and cross-linker between GO sheets through these various electrostatic attractions, ultimately resulting in the formation of an extended layer-type structure. X-ray diffraction (XRD) data reveals a slight increase in the interplanar spacing of the GO sheets, from 8.86 Å (for pure GO) to 8.98 Å (for GO-MTX), indicating the formation of an extended layer-type structure due to strong interactions between GO sheets and mitoxantrone binder molecules. This extended layer structure further self-assembles to create a robust 3D network structure comprising nanosheets and nanofibers through non-covalent interactions. This observation is corroborated by morphological analyses. Rheological studies demonstrate that an

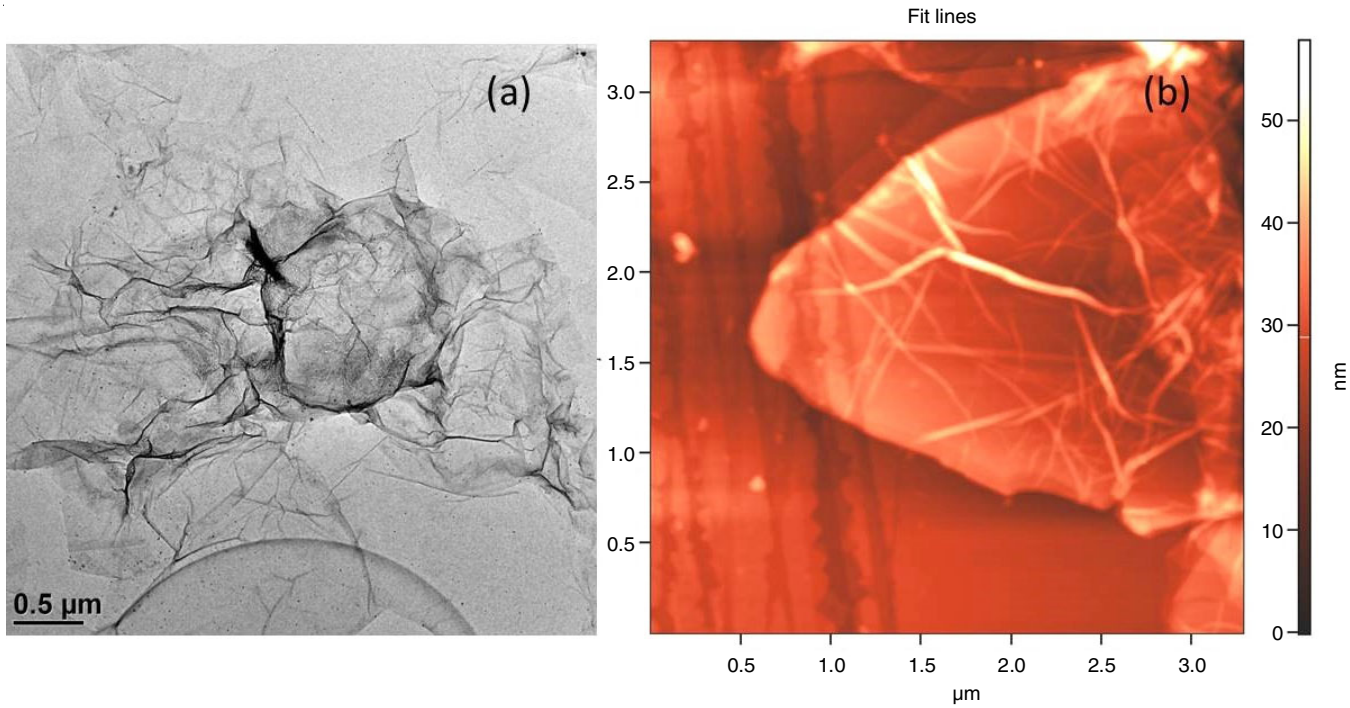

Fig. 4. (a) TEM image and (b) AFM image of GO-MTX gel

increase in mitoxantrone (binder) concentration significantly enhances the mechanical strength of gel. The storage modulus (G′) of the gel-phase material experiences a notable increase as binder concentration is raised from 0.36 to 0.54% (w/v). This strengthening is attributed to the development of a more robust 3D network structure in the gel phase, resulting from increased crosslinking between GO sheets and mitoxantrone binder molecules. Consequently, the water molecules become immobilized within this 3D network structure, giving rise to the formation of the gel.

Drug release studies: It has been well known that Ca^{2+} can bind readily to oxygen functional groups. Graphene oxide (GO) contains many oxygen functionalities (-OH, -COOH, epoxide) and therefore, Ca^{2+} can strongly bind to these hydroxyl, epoxide and carboxylic functional groups of GO. Ruoff *et al.* [35] described that divalent ion (Ca^{2+}, Mg^{2+}) act as a good crosslinking agent between GO sheet through binding with hydroxyl and carboxylic functional groups of GO. This leads to the increases the mechanical strength of the GO-based paper. Lately, Kinoshita *et al*. [34] harnessed the crosslinking ability of Ca^{2+} ions, facilitated by the presence of carboxyl groups, to induce calcium phosphate mineralization within peptide hydrogels. The study of this specific property of Ca^{2+} ions gives an idea about its ability to perform as a sustained and controlled release of other binding molecules (mitoxantrone) from GO-based gel. In present work, at first, the GO-MTX gel was prepared in a glass vial. A fixed amount (0.19%, w/v) of Ca^{2+} solutions has been added to the gel. The resulting solution was kept undisturbed for about a few minutes. After a few minutes, a small sample of solution was periodically withdrawn for UV-visible spectroscopic experiment at different time intervals and the absorbance values at 609 nm for mitoxantrone were consistently measured. This experiment confirmed the slow release of drug molecules from the GO-based gel. It is also important that the released drug molecules must retain their structure and activity to make the gel a successful drug delivery agent. The UV-visible spectroscopic results imply the released mitoxantrone and the pure mitoxantrone are almost similar. Therefore, it can be said that the structure of mitoxantrone is retained even after release. The percentage release profile of drugs with error bars (Fig. 5a) shows up to 26% release of the drug molecule for up to 24 h.

With an increase in the concentration of Ca^{2+} (0.42%, w/v), the release rate enhances significantly and about 95% of the drug molecules release from the gel in 13 h (Fig. 5c). In this case, the strength of the gel has slightly decreased compared with that of the previous gel. It may be interpreted as in the GO-MTX gel, three types of electrostatic interactions namely hydrogen bonding, acid–base and π–π stacking have been present, which causes the formation of gel-type materials. Nonetheless, the introduction of Ca^{2+} ions leads to a strong association with carboxylic acid groups located at the periphery of individual GO sheets, thereby inducing crosslinking between adjacent sheets. Moreover, Ca^{2+} ions (Lewis acidic metal ions) can open the epoxides ring to create C–OH bonds. All these types of strong bonding interactions facilitate the intercalation of the Ca^{2+} ions into the GO sheets and a corresponding release

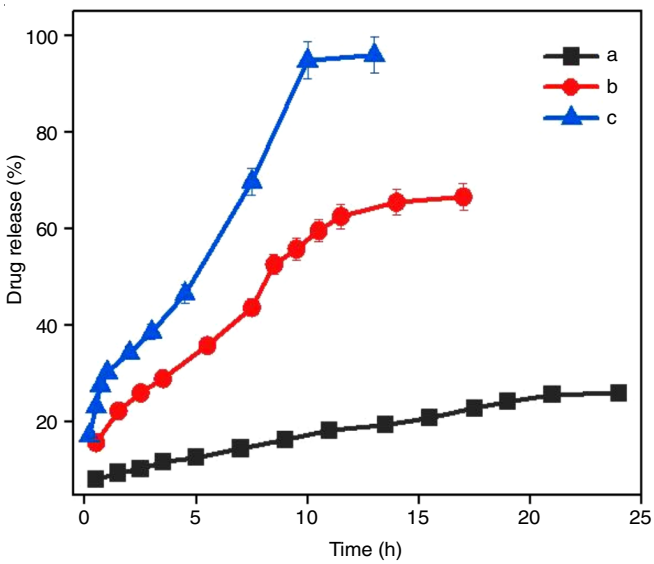

Fig. 5. Percentage release plot of mitoxantrone drug from the GO-MTX gel by the addition of Ca^{2+} solution where the concentration of the added Ca^{2+} was (a) 0.19% (w/v), (b) 0.28% (w/v) and (c) 0.42% (w/v)

of the mitoxantrone molecules. Thus, the replacement of the weak bonding interactions (between GO and mitoxantrone) with strong bond formation (between GO and Ca^{2+} ions) results in the corresponding decrease of the gel strength. At high concentrations of Ca^{2+} ions, most of the GO sheets are involved in crosslinked with Ca^{2+} ions with subsequent release of drug molecules. This results in the high release of mitoxantrone with the lower viscoelastic property of the gel. Under optimum concentration of Ca^{2+} (0.28%, w/v), the gel matrices show up to 66% release of the molecule for up to 17 h (Fig. 5b). Hence, the concentration of Ca^{2+} ions plays a pivotal role in dictating the drug-release behaviour of the gel samples. This present study describes the use of this GO-based gel system as a short-term delivery device for control release of anticancer drug (mitoxantrone) and can be suitable for tailored medical treatment in future.

Conclusion

To sum up, a straightforward and effective approach has been devised for synthesizing a gel based on graphene oxide (GO) by incorporating the anticancer drug mitoxantrone. The mitoxantrone molecule can act as a crosslinking/binding agent that can bind to the GO and result in the formation of a gel. The gel formation can be readily understood in terms of non-covalent interactions including hydrogen bonding, π–π stacking and acid–base type interactions. By introducing a minimal quantity of Ca^{2+} metal ions into the gel, this GO-based gel provides a controlled and prolonged release mechanism for mitoxantrone molecules. The Ca^{2+} metal ions intercalate into the GO sheet easily as the strong binding affinity of the divalent metal ions with the GO and subsequent release of mitoxantrone. Anticipated future research into this approach, along with adjustments to the concentration of these divalent ions, holds the potential to yield a novel category of GO-based materials with promising applications in the medical domain.

ACKNOWLEDGEMENTS

The author extends heartfelt appreciation to Krishnagar Government College, Krishnagar, India, for their generous provision of research resources. Furthermore, gratitude is also expressed to the Indian Association for the Cultivation of Sciences (IACS), India, for their invaluable support in granting access to the instrumental facilities and their extensive library resources.

CONFLICT OF INTEREST

The authors declare that there is no conflict of interests regarding the publication of this article.

REFERENCES

1. K.Y. Lee and D.J. Mooney, *Chem. Rev.*, **101**, 1869 (2001); https://doi.org/10.1021/cr000108x
2. A.R. Hirst, B. Escuder, J.F. Miravet and D.K. Smith, *Angew. Chem. Int. Ed.*, **47**, 8002 (2008); https://doi.org/10.1002/anie.200800022
3. X. Li, K. Yi, J. Shi, Y. Gao, H.-C. Lin and B. Xu, *J. Am. Chem. Soc.*, **133**, 17513 (2011); https://doi.org/10.1021/ja208456k
4. A.M. Kloxin, M.W. Tibbitt and K.S. Anseth, *Nat. Protoc.*, **5**, 1867 (2010); https://doi.org/10.1038/nprot.2010.139
5. S. Basak, J. Nanda and A. Banerjee, *J. Mater. Chem.*, **22**, 11658 (2012); https://doi.org/10.1039/c2jm30711a
6. S.S. Babu, V.K. Praveen and A. Ajayaghosh, *Chem. Rev.*, **114**, 1973 (2014); https://doi.org/10.1021/cr400195e
7. A. Baral, S. Roy, A. Dehsorkhi, I.W. Hamley, S. Mohapatra, S. Ghosh and A. Banerjee, *Langmuir*, **30**, 929 (2014); https://doi.org/10.1021/la4043638
8. M. Mba, A.I. Jiménez and A. Moretto, *Chem. Eur. J.*, **20**, 3888 (2014); https://doi.org/10.1002/chem.201304912
9. J. Nanda, A. Biswas, B. Adhikari and A. Banerjee, *Angew. Chem. Int. Ed.*, **52**, 5041 (2013); https://doi.org/10.1002/anie.201301128
10. A. Biswas and A. Banerjee, *Soft Matter*, **11**, 4226 (2015); https://doi.org/10.1039/C5SM00359H
11. S. Hussain and S.S. Maktedar, *Results Chem.*, **6**, 101029 (2023); https://doi.org/10.1016/j.rechem.2023.101029
12. L. Cao, Y. Liu, B. Zhang and L. Lu, *ACS Appl. Mater. Interfaces*, **2**, 2339 (2010); https://doi.org/10.1021/am100372m
13. M.J. Allen, V.C. Tung and R.B. Kaner, *Chem. Rev.*, **110**, 132 (2010); https://doi.org/10.1021/cr900070d
14. B. Adhikari, A. Biswas and A. Banerjee, *ACS Appl. Mater. Interfaces*, **4**, 5472 (2012); https://doi.org/10.1021/am301373n
15. S. Bae, H. Kim, Y. Lee, X. Xu, J.-S. Park, Y. Zheng, J. Balakrishnan, T. Lei, H. Ri Kim, Y.I. Song, Y.-J. Kim, K.S. Kim, B. Özyilmaz, J.-H. Ahn, B.H. Hong and S. Iijima, *Nat. Nanotechnol.*, **5**, 574 (2010); https://doi.org/10.1038/nnano.2010.132
16. X. Zhou, Y. Wei, Q. He, F. Boey, Q. Zhang and H. Zhang, *Chem. Commun.*, **46**, 6974 (2010); https://doi.org/10.1039/c0cc01681k
17. X. Huang, X. Qi, F. Boey and H. Zhang, *Chem. Soc. Rev.*, **41**, 666 (2012); https://doi.org/10.1039/C1CS15078B
18. S. Bi, T. Zhao and B. Luo, *Chem. Commun.*, **48**, 106 (2012); https://doi.org/10.1039/C1CC15443E
19. Y. Wang, Z. Li, J. Wang, J. Li and Y. Lin, *Trends Biotechnol.*, **29**, 205 (2011); https://doi.org/10.1016/j.tibtech.2011.01.008
20. J. Ma, J. Zhang, Z. Xiong, Y. Yong and X.S. Zhao, *J. Mater. Chem.*, **21**, 3350 (2011); https://doi.org/10.1039/C0JM02806A
21. B.G. Choi, H. Park, M.H. Yang, Y.M. Jung, S.Y. Lee, W.H. Hong and T.J. Park, *Nanoscale*, **2**, 2692 (2010); https://doi.org/10.1039/c0nr00562b
22. J. Zhu, T. Zhu, X. Zhou, Y. Zhang, X.W. Lou, X. Chen, H. Zhang, H.H. Hng and Q. Yan, *Nanoscale*, **3**, 1084 (2011); https://doi.org/10.1039/C0NR00744G
23. C.N.R. Rao, A.K. Sood, R. Voggu and K.S. Subrahmanyam, *J. Phys. Chem. Lett.*, **1**, 572 (2010); https://doi.org/10.1021/jz9004174
24. S.K. Tiwari, S. Sahoo, N. Wang and A. Huczko, *J. Science: Adv. Mater. Devices*, **5**, 10 (2020); https://doi.org/10.1016/j.jsamd.2020.01.006
25. W. Gao, M. Majumder, L.B. Alemany, T.N. Narayanan, M.A. Ibarra, B.K. Pradhan and P.M. Ajayan, *ACS Appl. Mater. Interfaces*, **3**, 1821 (2011); https://doi.org/10.1021/am200300u
26. V. Chandra and K.S. Kim, *Chem. Commun.*, **47**, 3942 (2011); https://doi.org/10.1039/c1cc00005e
27. Y. Tang, H. Guo, L. Xiao, S. Yu, N. Gao and Y. Wang, *Colloids Surf. A: Physicochem. Eng. Asp.*, **424**, 74 (2013); https://doi.org/10.1016/j.colsurfa.2013.02.030
28. S. Sattari, M. Adeli, S. Beyranvand and M. Nemati, *Int. J. Nanomedicine*, **16**, 5955 (2021); https://doi.org/10.2147/IJN.S249712
29. R. Li, Y. Wang, J. Du, X. Wang, A. Duan, R. Gao, J. Liu and B. Li, *Sci. Rep.*, **11**, 1725 (2021); https://doi.org/10.1038/s41598-021-81218-3
30. J.N. Tiwari, K. Mahesh, N.H. Le, K.C. Kemp, R. Timilsina, R.N. Tiwari and K.S. Kim, *Carbon*, **56**, 173 (2013); https://doi.org/10.1016/j.carbon.2013.01.001
31. D. Ma, J. Lin, Y. Chen, W. Xue and L.-M. Zhang, *Carbon*, **50**, 3001 (2012); https://doi.org/10.1016/j.carbon.2012.02.083
32. X. Yang, X. Zhang, Z. Liu, Y. Ma, Y. Huang and Y. Chen, *J. Phys. Chem. C*, **112**, 17554 (2008); https://doi.org/10.1021/jp806751k
33. H. Kim, D. Lee, J. Kim, T. Kim and W.J. Kim, *ACS Nano*, **7**, 6735 (2013); https://doi.org/10.1021/nn403096s
34. T. Nonoyama, H. Ogasawara, M. Tanaka, M. Higuchi and T. Kinoshita, *Soft Matter*, **8**, 11531 (2012); https://doi.org/10.1039/c2sm26538a
35. S. Park, K.-S. Lee, G. Bozoklu, W. Cai, S.T. Nguyen and R.S. Ruoff, *ACS Nano*, **2**, 572 (2008); https://doi.org/10.1021/nn700349a
36. W. Hummers Jr. and R.E. Offeman, *J. Am. Chem. Soc.*, **80**, 1339 (1958); https://doi.org/10.1021/ja01539a017
37. Q. Zhuo, J. Gao, M. Peng, L. Bai, J. Deng, Y. Xia, Y. Ma, J. Zhong and X. Sun, *Carbon*, **52**, 559 (2013); https://doi.org/10.1016/j.carbon.2012.10.014